JOURNAL OF PLANKTON RESEARCH | VOLUME 32 | NUMBER 2 | PAGES 181–195 | 2010

Primary production in the Argentine Sea during spring estimated by field and satellite models

VIVIAN A. LUTZ[1,2]*, VALERIA SEGURA[1], ANA I. DOGLIOTTI[2,3,4], DOMINGO A. GAGLIARDINI[2,3,5], ALEJANDRO A. BIANCHI[6] AND CARLOS F. BALESTRINI[6]

[1]INSTITUTO NACIONAL DE INVESTIGACIÓN Y DESARROLLO PESQUERO, PASEO VICTORIA OCAMPO NO 1, MAR DEL PLATA B7602HSA, ARGENTINA, [2]CONSEJO NACIONAL DE INVESTIGACIONES CIENTÍFICAS Y TÉCNICAS, ARGENTINA, [3]INSTITUTO DE ASTRONOMÍA Y FÍSICA DEL ESPACIO (IAFE-CONICET), PABELLÓN IAFE-CIUDAD UNIVERSITARIA, C.C. 67- SUC. 28 (1428), BUENOS AIRES, ARGENTINA, [4]DEPARTMENT OF PHYSICS, FEDERAL UNIVERSITY OF RIO GRANDE, AV. ITALIA, KM 8, RIO GRANDE RS 96201-900, BRAZIL, [5]CENTRO NACIONAL PATAGÓNICO (CENPAT-CONICET), BOULEVARD BROWN S/N, PUERTO MADRYN, ARGENTINA AND [6]DEPARTAMENTO OCEANOGRAFÍA, SERVICIO DE HIDROGRAFÍA NAVAL, AV. MONTES DE OCA 2124, 1271 BUENOS AIRES, ARGENTINA

*CORRESPONDING AUTHOR: vlutz@inidep.edu.ar

Received August 28, 2009; accepted in principle October 22, 2009; accepted for publication October 31, 2009

Corresponding editor: William Li

In satellite images of the world ocean the Argentine Sea is one of the areas of highest chlorophyll-*a* (Chl *a*) concentration. Here we analyze the spatial variability in primary production in relationship to phytoplankton biomass, and some relevant optical and physical characteristics observed during spring 2005. High Chl *a* concentrations were found in frontal areas, mainly at the shelf-break (19.0 mg m^{-3}) and Grande Bay (28.6 mg m^{-3}), with the lowest values offshore (0.4 mg m^{-3}). Integrated production also varied widely from ~275 to 5480 mg C m^{-2} d^{-1}. Variations in the Chl *a*/in vivo-fluorescence, and photosynthetic parameters were related to the absorption characteristics of phytoplankton, indicating the influence of variations in the phytoplankton community composition. Surface Chl *a* explained only 51% of the variance in integrated primary production. Neither integrated production, nor the photosynthetic parameters were significantly related to seawater temperature. The simple satellite model used here resulted in significant underestimation of field primary production values (Absolute Percentage Difference > 50%). Our results indicate that a more adequate satellite model of production, making use of local photosynthetic parameters and vertical distribution of biomass, should be developed for this region.

INTRODUCTION

The Argentine shelf and its shelf-break constitute one of the richest biological areas of the world oceans. Commercially important species of fish and molluscs (Cousseau and Perrota, 2000), as well as seabirds and marine mammals (Campagna *et al.*, 1998) are important in this region. Global studies using ocean-color satellite images have revealed bright features denoting high chlorophyll concentrations, which translated into high rates of carbon turnover when primary production models were applied (Longhurst *et al.*, 1995). Moreover, in a global study, Gregg *et al.* (Gregg *et al.*, 2005) estimated that this is the region with the highest increase in chlorophyll during the period considered (1998–2003). The region also makes an important contribution to the global ocean CO_2 uptake from the atmosphere (Bianchi *et al.*, 2009).

The Argentine Sea is characterized by the presence of several oceanic and coastal frontal systems. In the study area tidal (e.g. off Valdés Peninsula), coastal (e.g. Grande Bay), as well as the shelf-break (coincident with the external shelf border) fronts are distinct features and their relevance for the distribution of phytoplankton has long been recognized (Carreto *et al.*, 1986, 2007; Negri *et al.*, 1992).

The use of ocean-color satellite images in this region has increased over the past decade. The pioneering study by Brown and Podestá (Brown and Podestá, 1997)

doi:10.1093/plankt/fbp117, available online at www.plankt.oxfordjournals.org. Advance Access publication November 28, 2009

Table I: Symbols used and their corresponding units

Notation	Description	Units
$a_d(\lambda)$	Absorption coefficient of detritus at wavelength (λ)	m^{-1}
$a_{ph}(\lambda)$	Absorption coefficient of phytoplankton at wavelength (λ)	m^{-1}
$a_{ph}^B(\lambda)$	$a_{ph}(\lambda)$ normalized by Chl *a*	m^2 (mg Chl *a*)$^{-1}$
$a_t(\lambda)$	Absorption coefficient of total particulate matter at wavelength (λ)	m^{-1}
α	Initial slope of production versus irradiance (at low values)	mg C h^{-1}[μmol quanta m^{-2} s^{-1}]$^{-1}$ or mg C h^{-1} [W m^{-2}]$^{-1}$
α^B	α normalized by Chl *a*	mg C [mg Chl *a*]$^{-1}$ h^{-1}[μmol quanta m^{-2} s^{-1}]$^{-1}$ or mg C [mg Chl *a*]$^{-1}$ h^{-1}[W m^{-2}]$^{-1}$
B	Phytoplankton biomass as Chl *a*	mg m^{-3}
D	Length of daylight	h
I_0	Irradiance at surface	μmol quanta m^{-2} s^{-1}
$I(z)$	Irradiance at depth z	μmol quanta m^{-2} s^{-1}
$I(z, t)$	Irradiance at depth z and time t	μmol quanta m^{-2} s^{-1}
I_0^m	Surface irradiance at local noon	μmol quanta m^{-2} s^{-1} or W m^{-2}
I_k	Photoadaptation parameter, [P_m/α]	μmol quanta m^{-2} s^{-1} or W m^{-2}
I_*^m	Non-dimensional irradiance, [I_0^m/I_k]	Dimensionless
K_d(PAR)	Diffuse attenuation coefficient for downwelling irradiance	m^{-1}
Ω_x	Weights for the polynomial approximation to [I_*^m]	Dimensionless
p	Instantaneous production	mg C m^{-3} h^{-1}
$p^B(z)$	Instantaneous production normalized by Chl *a* at depth z	mg C [mg Chl *a*]$^{-1}$ h^{-1}
P_m	Maximum production at saturating irradiance	mg C h^{-1}
P_m^B	P_m normalized by Chl *a*	mg C [mg Chl *a*]$^{-1}$ h^{-1}
$P_{Z,T}$	Daily water column primary production	mg C m^{-2} d^{-1}
T	Time	h

suggesting the presence of coccolithophorids at the shelf-break has recently been followed by that of Signorini *et al.* (Signorini *et al.*, 2006). Some studies have been made on differences between *in situ* and satellite chlorophyll estimates (Lutz *et al.*, 2006; Dogliotti *et al.*, 2009), and others, based solely on satellite information, have analyzed the annual patterns of chlorophyll distribution (Rivas *et al.*, 2006; Romero *et al.*, 2006). Garcia *et al.* (Garcia *et al.*, 2005) tested the efficiency of local algorithms, and Gonzalez-Silvera *et al.* (Gonzalez-Silvera *et al.*, 2004) attempted a first classification into sub-regions according to variations in the ocean-color signal.

Regarding field estimates of primary production, however, the information remains scarce. The first extensive study (Argentine shelf and Antarctica) of primary production (instantaneous values) was performed during 1962–1965. These results (Mandelli, 1965; El-Sayed, 1967) showed that production was higher at the north than at the south of the shelf-break at the beginning of the spring bloom, and that the efficiency of production per unit chlorophyll increased as the season progressed. A recent study by Schloss *et al.* (Schloss *et al.*, 2007) describes large variations in primary production (instantaneous values) in different areas of the shelf and shelf-break for summer and autumn in connection with variations in CO_2 uptake. Another recent work by Garcia *et al.* (Garcia *et al.*, 2008) reports high values of primary production at four locations at the shelf-break associated with the spring bloom.

Models most commonly used to estimate primary production at sea require as input: chlorophyll-*a* (Chl *a*) concentration and light intensity; and the photosynthetic parameters α, the initial slope at low irradiances, and P_m (see notations in Table I), the maximum production at saturating irradiance (Platt *et al.*, 1980). The magnitudes of surface chlorophyll and light can nowadays be estimated through remote sensing. On the other hand, the photosynthetic parameters have to be determined by performing some specific *in situ* experiments, usually a production versus irradiance incubation. Due to the lack of values of the photosynthetic parameters for the southwestern Atlantic region, global models of primary production still rely on the use of fixed parameters extracted from other archived data measured elsewhere in the world ocean.

The aims of this work were to investigate spatial variations in the primary production in an extensive area of the Argentine Sea during spring, using field estimated photosynthetic parameters, and to compare the outputs of a standard satellite model of primary production against these field results. We analyzed the distribution of Chl *a* (*in situ* and satellite) and the relationship between phytoplankton physiological parameters and some environmental and optical variables to understand the variations observed in primary production.

METHOD

Sampling

Sampling was performed in the Argentine Sea (from 38 to 55° S and 55° W to the coast) on board the RV "ARA Puerto Deseado" between the 8 and the 28 of October

2005 (Fig. 1; color image available as Supplementary Data). Eight vertically resolved transects were included (Fig. 1; color image available as Supplementary Data). At all stations continuous profiles of temperature and salinity were determined using a Sea-Bird 911 CTD, and *in vivo* active fluorescence measured by a Sea-Point fluorometer attached to the CTD. At 41 stations (marked with crosses in Fig. 1; color image available as Supplementary Data) surface water samples were collected using a bucket, and at two or three selected depths using Niskin bottles. These samples were used for determination of Chl *a* and particulate absorption. At 22 stations (marked with circles in Fig. 1; color image available as Supplementary Data) surface samples were used to run production versus irradiance incubation experiments.

In vivo active fluorescence was measured along the ship track, by a Model 10-005R Turner Designs fluorometer connected to a flow-through system (pumping water from the subsurface ~3.5 m). Photosynthetically-active-radiation (PAR, 400–700 nm) at the surface, I_o (see notations in Table I), was monitored continuously during the whole cruise with a cosine downwelling irradiance (LI-COR) sensor.

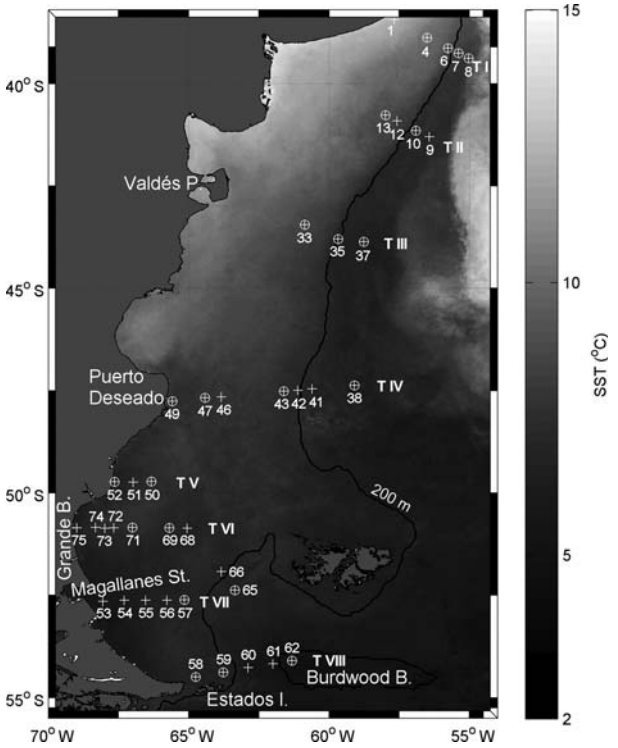

Fig. 1. SST distribution from MODIS-Aqua October 2005 monthly (4 km) composite. The location and ID-number of the stations (8–28 October) are shown. Crosses indicate stations with vertical profiles of Chl *a*; circles indicate sites where surface P&I incubations were run. Transect numbers are also shown.

Chl *a* concentration

Immediately after collection seawater samples were filtered, under dim light and low pressure (<35 kPa), onto Millipore APFF (similar to Whatman GF/F) glass-fiber-filters. These filters were kept in liquid nitrogen (−196°C) on board and in an ultra-freezer (−86°C) in the laboratory until analysis. A modification of the fluorometric method (Holm-Hansen *et al.*, 1965) was used to determine the Chl *a* concentrations. Pigments on filters were extracted in 100% methanol, disrupted with a probe-sonicator, and kept overnight in the freezer; after this they were stirred in a vortex, and centrifuged. Fluorescence from the supernatant extract was read in a spectrofluorometer Perkin Elmer LS3 (excitation and emission wavelengths 430 and 666 nm, respectively). The spectrofluorometer was previously calibrated with standard Chl *a* (Sigma, from cyanobacteria), which was first dissolved in 100% acetone (since methylation may alter the pigments kept for long time in methanol), and the concentration of this work-solution determined in a spectrophotometer (using the extinction coefficients from Jeffrey and Humphrey, 1975); from this concentrated work-solution dilutions in 100% methanol (taking care that acetone was <3% of the final solution) were prepared to run the calibration curve in the spectrofluorometer. No acidification was performed in the analysis of the samples, since the use of a Chl *a* specific set of wavelengths avoids the interference by phaeopigments and other chlorophylls in the sample.

The values of Chl *a* concentration rendered by 100% methanol and by the classic 90% acetone acidification method (Holm-Hansen *et al.*, 1965) were compared in 20 replicate surface samples (Fig. 2). Although the correlation between Chl *a* values retrieved by the two solvents was good ($r^2 = 0.96$), the concentration of samples with low Chl *a* (expected to have a higher proportion of small, difficult-to-extract species) was significantly higher using 100% methanol (>30% in 10 out of 20 samples). This better efficiency of 100% methanol extraction was already shown by Holm-Hansen and Riemann (Holm-Hansen and Riemann, 1978) and confirmed in a recent comparison for the fluorometric technique (Lutz *et al.*, 2007), as well as in a comparison exercise for the HPLC method (Wright *et al.*, 1997).

In vivo fluorescence and Chl *a*

Surface

The performance of the flow-through fluorometer was tested by measuring dilutions from a single flask (i.e.

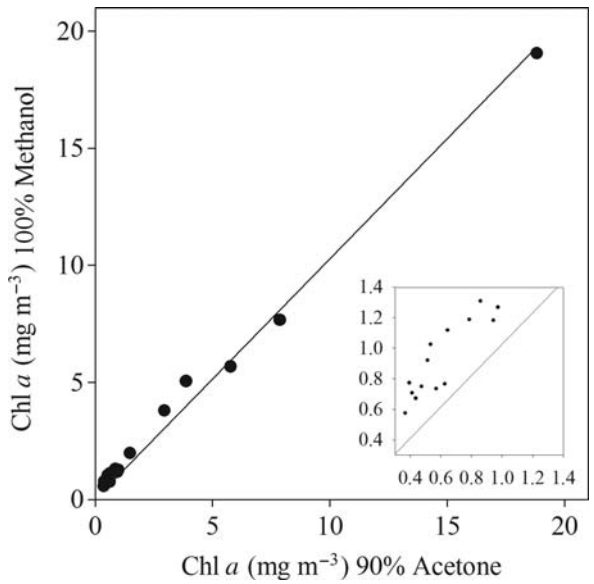

Fig. 2. Regression between the efficiency of Chl *a* extraction by 90%-acetone versus that by 100%-methanol. Surface samples from 20 stations were used for this analysis. The insert shows expanded axes for low Chl *a* concentrations.

same growth conditions) of a culture of *Emiliania huxleyi* which showed a linear response between fluorescence and Chl *a* concentration ($r^2 = 0.96$). This is the only case, same species and same physiological status, where such a linear response would be expected between *in vivo* fluorescence and Chl *a*. In this way we could verify that fluctuations observed in the Ch1 *a/in vivo* fluorescence (CF) ratio at the surface, along the cruise, represented real natural variations. Between stations, seawater samples for analysis of Chl *a* were taken approximately every 2 h (or whenever there was a marked change in fluorescence) from the flow-through system (see points in Fig. 3a; color image available as Supplementary Data).

Vertical profiles

The fluorescence profiles were converted into Chl *a* concentration by calculating the CF ratio at depths where Chl *a* samples were analyzed and linearly interpolating the CFs within these layers. Nevertheless, all profiles were carefully inspected and in some cases, where a clear photoinhibition effect was detected at the surface (see Results) Chl *a* concentrations were linearly interpolated from the actual Chl *a* values at the surface and at the second sampling depth.

Particulate absorption

The procedure used for filtration and storage of samples was the same used for the Chl *a* samples. For the analysis the quantitative filter technique of Mitchell (Mitchell, 1990) was followed, using a UV-2450 Shimadzu spectrophotometer with an integrating sphere. The absorption coefficients of total particulate material [$a_t(\lambda)$] and of detritus [$a_d(\lambda)$] were obtained according to the quadratic equation of Mitchell (Mitchell, 1990), and the coefficients given by Hoepffner and Sathyendranath (Hoepffner and Sathyendranath, 1992), to correct for the pathlength amplification effect. The phytoplankton absorption coefficient, $a_{ph}(\lambda)$, was calculated by subtracting $a_d(\lambda)$ from $a_t(\lambda)$.

Downwelling irradiance profiles

The study area was divided every 2° into 9 latitudinal-ranks (LR), and in turn each one was divided every 2 h (during daylight) into 9 hour-ranks (HR). The average I_o from all the measurements recorded by the continuous sensor within the same LR and HR, were computed. The PAR downwelling attenuation coefficients, K_d(PAR), were obtained following the parameterization proposed by Sathyendranath and Platt (Sathyendranath and Platt, 1988). The inputs for the model were: the absorption and scattering spectra of pure seawater (Pope and Fry, 1997); the values of Chl *a*, $a_t(\lambda)$, and $a_{ph}(\lambda)$ obtained for discrete depths; and the corresponding average I_o. Using these values of K_d(PAR) per meter, the irradiance profiles for each HR, $I(z, t)$, were calculated. The accuracy of the parameterization used was tested for nine stations where *in situ* profiles of $I(z)$ were measured with a Biospherical PUV-500/510B radiometer; the average coefficient of variation between the modeled and measured values of K_d(PAR) at 5 m was CV = 15% ± 8%.

Field estimation of primary production

An incubation box with halogen lamps to hold 500-ml square polycarbonate Nalgene bottles, with a thermally regulated water circulation system, was specially designed. The stable mass isotope ^{13}C method followed was that of Hama *et al.* (Hama *et al.*, 1983). A surface seawater sample was inoculated with a solution of $NaH^{13}CO_3$ to a final enrichment of 8.02%, dispensed into 20 light and two dark bottles (as a control), and incubated for 3 h, maintaining the temperature close to that of the sea. A sample not inoculated was filtered at the beginning of the experiment for the determination of natural ^{13}C abundance in the water. After the incubation each bottle was filtered onto pre-combusted Whatman GF/F glass-fiber-filters. The filters were stored dry. In the laboratory, filters were fumed with HCl and encapsulated. The amount of ^{13}C in the samples was analyzed in a Delta Plus IRMS Thermo Finnigan mass spectrometer. Instantaneous production,

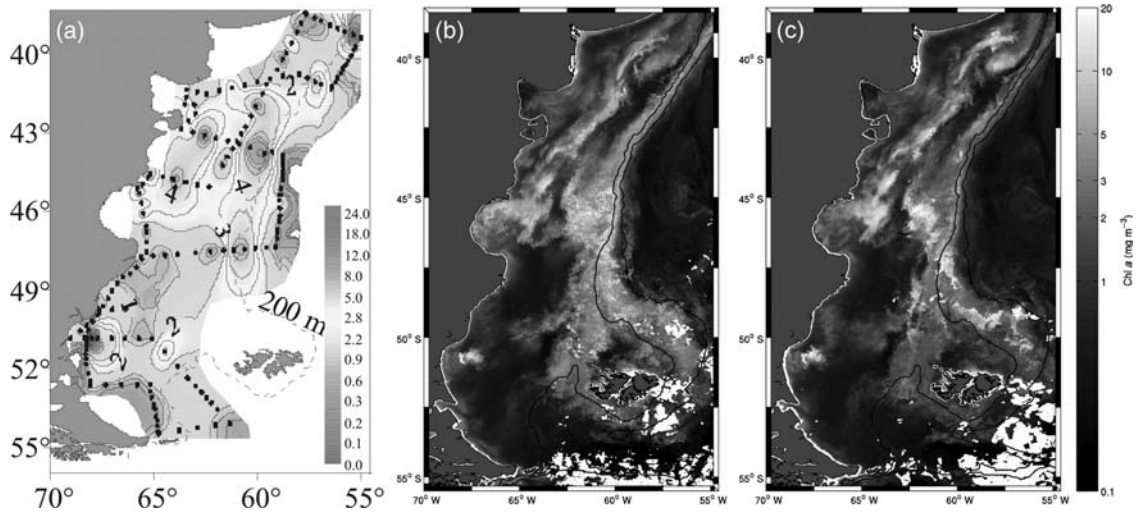

Fig. 3. Surface distribution of Chl *a* concentration (mg m^{-3}) in the Argentine Sea during spring 2005. (**a**) *In situ* measurements (dots show the sampling locations). Satellite estimations are 1 km resolution images averaged over the studied period (8–28 October 2005). (**b**) SeaWiFS (algorithm OC4v4); (**c**) MODIS (algorithm OC3M).

p, was computed according to the equations in Fernandez *et al.* (Fernandez *et al.*, 2005); which are modifications from Hama *et al.* (Hama *et al.*, 1983) and Collos and Slawyk (Collos and Slawyk, 1985).

The exponential equation of Platt *et al.* (Platt *et al.*, 1980) was used to fit the production versus irradiance curves and to obtain the photosynthetic parameters (α and P_m). After a first fitting, those points that deviated beyond two standard deviations were excluded, and a second fitting was run to get the final parameters (mean $r^2 = 0.94 \pm 0.06$, $n = 22$). α was corrected for the spectral composition of the incident light taking into account the spectrum of the lamp and the phytoplankton absorption spectrum of each sample (Dubinsky *et al.*, 1986). To estimate the instantaneous normalized production, $p^B(z)$ at depth z the exponential equation of Platt *et al.* (Platt *et al.*, 1980) was used. Daily primary production per unit area, $P_{Z,T}$ was finally computed by multiplying these values by the corresponding Chl *a* concentration and integrating them throughout the daylight (D) and the whole water column (i.e. ∞, since $p^B(z)$ would become zero when $I(z)$ becomes zero):

$$P_{Z,T} = \int_0^D \int_0^\infty B(z) p^B(I(z,t)) \mathrm{d}z \mathrm{d}t \qquad (1)$$

$B(z)$ were those obtained from the discrete Chl *a* measurements and the conversion of the continuous fluorescence profiles, and the assumption was that these would not change throughout the day. $I(z,t)$ were those computed for each depth for each HR. α^B and P_m^B were estimated for the surface at a given time, hence the assumption was that these would be fixed throughout the water column and the day.

Satellite data

MODIS (level 1A) and ancillary data from the sampled period were obtained from the ocean color website (http://oceancolor.gsfc.nasa.gov) and SeaWiFS Local Area Coverage (LAC) full resolution ($\sim$1 km) images (level 1A) were provided by CONAE (Comisión Nacional de Actividades Espaciales). Daily SeaWiFS and MODIS images were processed from level 1A to level 2 using SeaDAS (SeaWiFS Data Analysis System) Version 5.1.5. The standard atmospheric correction algorithms of SeaDAS were used and the following products were obtained: Chl *a*, using OC4v4 and OC3M algorithms for SeaWiFS and MODIS, respectively; PAR product, using the algorithm developed by R. Frouin (http://oceancolor.gsfc.nasa.gov/DOCS/seawifs_par_wfigs.pdf); and K_d(PAR) using the model of Morel *et al.* (Morel *et al.*, 2007).

Satellite estimation of primary production

The model of Platt and Sathyendranath (Platt and Sathyendranath, 1993) was used to estimate daily water column primary production using satellite information. In this first approach, the most standard, non-spectral and considering a vertically homogeneous biomass profile, model was used. This assumes a sinusoidal irradiance distribution throughout the day. The following representation of the analytic solution using a

polynomial approximation (Platt and Sathyendranath, 1993) was used (see notations in Table I):

$$P_{Z,T} = \frac{BP_m^B D}{K_d}\left[\sum_{x=1}^{5} \Omega_x \left(I_*^m\right)^x\right] \quad (2)$$

The values of B and K_d(PAR) were the products obtained from the satellite image analyses, surface irradiance at noon was calculated from satellite PAR product, daylight [D] was calculated as a function of latitude and time of year, and the photosynthetic parameters were those given by Longhurst *et al*. (Longhurst *et al*., 1995) for spring in the "Southwestern Atlantic province" ($\alpha^B = 0.086$ mg C [mg Chl a]$^{-1}$ h^{-1} [W m^{-2}]$^{-1}$; $P_m^B = 2.74$ mg C [mg Chl a]$^{-1}$ h^{-}). Ω_x are the weights for the polynomial approximation to [I_*^m]. In this first approach we assumed that B and K_d(PAR) were constant in the water column and throughout the day, and that α^B and P_m^B were constant vertically, temporally, and spatially for the studied area.

Composite $P_{Z,T}$ maps, using satellite products for each sensor (SeaWiFS and MODIS), were obtained averaging daily mapped $P_{Z,T}$ images (at ~1 km pixel resolution) over the sampled period. Field estimates were compared with: (1) daily satellite-derived $P_{Z,T}$ values; and (2) the value of the composite $P_{Z,T}$ image. In the first case the excluding criteria used was the same as in Dogliotti *et al*. (Dogliotti *et al*., 2009), but here the temporal window between the sampling and satellite overpass was $\pm$12 h. In the second case the nearest pixel to the sampled site was used in the match-up. Standard Major Axis type II regression model was used to compute the slope, intercept and the coefficient of determination of a linear equation that relates log-transformed field and satellite-derived $P_{Z,T}$ values.

RESULTS

Sea surface distributions of temperature (satellite) and Chl *a* (field and satellite)

Figure 1 (color image available as Supplementary Data) shows a composite satellite image of sea surface temperature, SST, denoting some main features: (1) a monthly signal of the cold Malvinas Current running along the shelf-break (close to the 200 m isobath); (2) two warm areas in the north (a strip of coastal waters; and another region offshore the Malvinas Current); and (3) the shelf slightly cooler towards the south.

In situ surface Chl *a* showed a wide range of variation from 0.4 to 28.6 mg m^{-3} (Fig. 3a; color image available as Supplementary Data). Phytoplankton blooms were developing along the shelf-break frontal area, with values of Chl *a* up to 19.0 mg m^{-3} in the north. Another region of high Chl *a* concentrations (>8.0 mg m^{-3}) appeared on the shelf off Valdés Peninsula probably associated with the tidal front in this area (Carreto *et al*., 1986). In the south a bloom was associated with the coastal front of Grande Bay (Sabatini *et al*., 2004), where the highest value of Chl *a* for the whole cruise (28.6 mg m^{-3}) was observed. Apart from these bloom areas, the shelf showed a background of medium Chl *a* values, mostly ~1.0 mg m^{-3}, whereas the lowest Chl *a* values were found on the south offshore from the shelf-break.

Satellite-derived Chl *a* distributions (Fig. 3b and c; color image available as Supplementary Data) resembled the main features depicted by *in situ* measurements (Fig. 3a; color image available as Supplementary Data), i.e. high values associated to tidal, coastal, and shelf-break fronts, and low values east of the shelf-break. Nevertheless, both SeaWiFS and MODIS derived Chl *a* underestimated *in situ* values. SeaWiFS values for coincidental match-ups ranged between 0.2 and 17.4 mg m^{-3}, although MODIS estimates were slightly lower.

Vertical distribution of Chl *a* (field)

Chl *a* profiles along the transects are shown in Fig. 4 (color image available as Supplementary Data). *Transect I* presented one of the highest spots of the shelf-break bloom, with Chl *a* concentrations (>15.0 mg m^{-3}) extending to depth (up to ~100 m); station 4 on the middle shelf had much lower Chl *a* concentrations (<1.5 mg m^{-3}) at the upper layer decreasing sharply below 50 m; and the coastal station showed a homogeneous profile (Chl *a* ~ 1.1 mg m^{-3}). *Transect II* showed the shelf-break bloom with a shallower distribution (<50 m), and lower Chl *a* concentrations on the shelf side, being homogeneous at St. 13 located in the middle shelf. *Transect III* showed low Chl *a* at stations 33 and 37 (located in the middle shelf and offshore respectively) and the highest values at station 35 at the shelf-break (Chl *a* ~ 10.0 mg m^{-3} at the top layer). *Transect IV* showed the shelf-break bloom at station 41 (Chl *a* > 10.0 mg m^{-3} at the top layer), and lower Chl *a* values at stations in the middle shelf and offshore. *Transect V*, a short one close to the coast up north from the outflow of the Santa Cruz River, showed no particular features, with moderate and relatively homogeneous Chl *a* values (~1.3 mg m^{-3}). *Transect VI* was located in Grande Bay in the middle of which an intensive and shallow (above ~ 30 m) bloom was detected (Chl *a* > 25.0 mg m^{-3}); Chl *a* values decreased closer to the

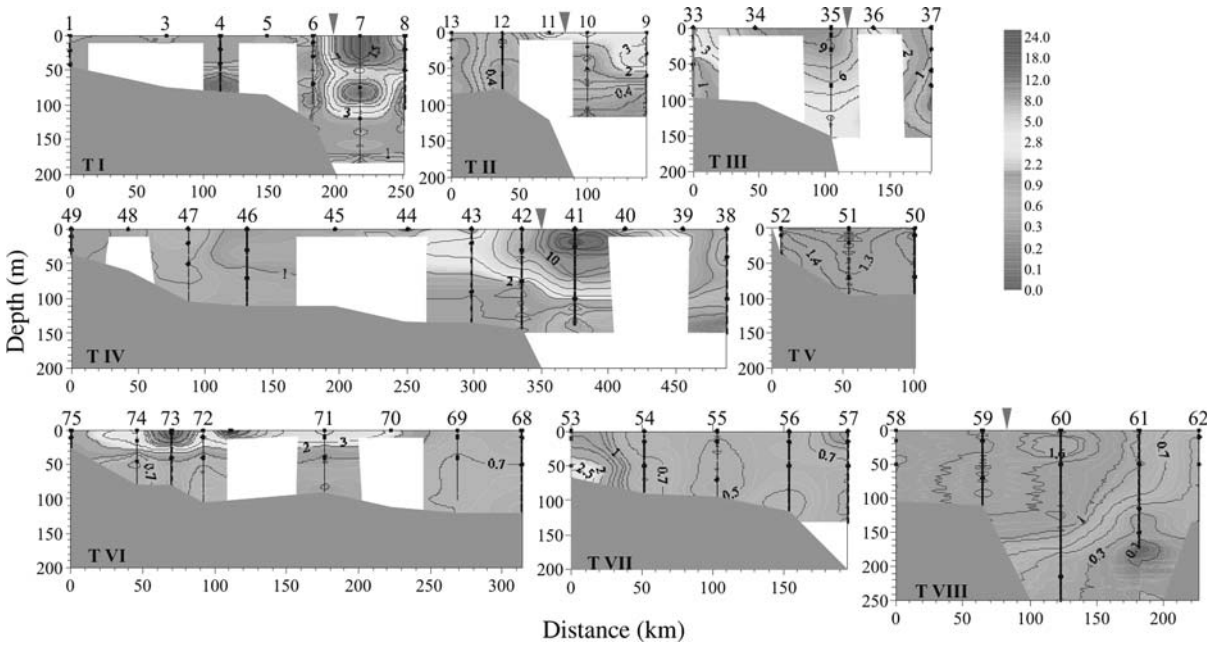

Fig. 4. Vertical distribution of Chl *a* (mg m^{-3}) on the eight transects studied (Fig. 1). Dots show depths for which Chl *a* analysis was performed, lines show Chl *a* values interpolated from *in vivo* fluorescence. Stations numbers are shown at the top; triangles mark the approximate position of the 200 m isobath. Blanks were left where no discrete Chl *a* analyses were performed at depth.

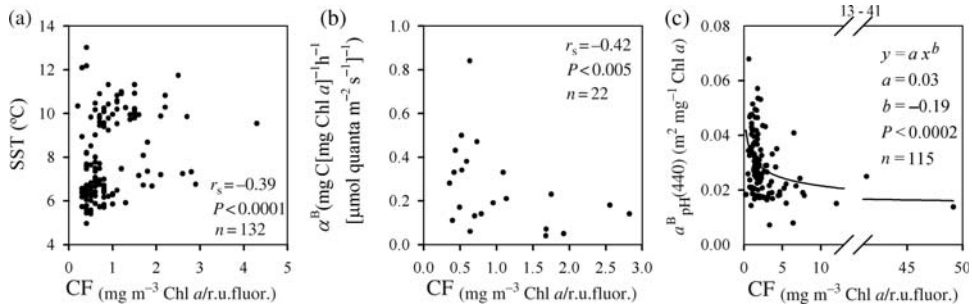

Fig. 5. Spearman correlation between the CF ratio at the surface and: (**a**) SST; (**b**) α^B. (**c**) Power function between CF at different depths and $a^B_{ph}(440)$.

coast and to the outer shelf area. *Transect VII* extended from the mouth of the Magallanes Strait showing high Chl *a* concentrations at depth close to the strait and at the surface on the outer shelf, and low Chl *a* (<0.8 mg m^{-3}) throughout the water column in the middle shelf. *Transect VIII* ran, slightly north of: Le Maire Strait, Los Estados Island into Burdwood Bank; Chl *a* values were medium on the West (~ 1.5 mg m^{-3}) and decreased towards depth and towards East (<0.3 mg m^{-3}).

Surface fluorescence

The relationship between *in vivo* fluorescence and Chl *a* concentrations was significant ($r^2 = 0.71$, $n = 132$). Nevertheless, the CF ratio showed a high variability with a mean of 0.91 ± 0.65 (coefficient of variation, CV, 67%). When studying the relationship between different variables, or physiological parameters, first the normality in the distribution of the data was checked (Kolmogorov–Smirnov test); if the two properties were normally distributed, the Pearson correlation, r_p, was used, otherwise the Spearman ranks correlation, r_s was used. The CF ratio showed a significant correlation with the sea surface temperature ($r_s = 0.39$; Fig. 5a), indicating that as temperature decreased the efficiency of fluorescence per unit Chl *a* increased (i.e. lower CF). For the 22 matching points CF also showed a significant negative correlation with α^B ($r_s = -0.42$; Fig. 5b); indicating that the efficiency of fluorescence per unit Chl *a* increased as α^B increased.

Fluorescence profiles

The relationship between *in vivo* fluorescence and Chl *a* with depth was also significant (r^2=0.86, $n = 115$). Nevertheless, the ratio CF in the vertical also showed a large variability (mean 3.40 ± 6.90, CV 203%). Part of this difference must be caused by differences in the instruments (for matching data the relationship between fluorescence-vertical and fluorescence-surface was $r^2 = 0.77$; $n = 28$), but part could also be attributed to natural variations. The CF showed a negative exponential relationship with the efficiency of absorption, $a^B_{ph}(440)$ (Fig. 5c). Another conspicuous variation in fluorescence in some profiles was evidence of photoinhibition at the surface, as shown in Fig. 6.

Photosynthetic parameters

A wide variation in the photosynthetic parameters was observed at the 22 stations studied; α^B ranged from 0.0096 to 0.182 mg C [mg Chl *a*]$^{-1}$ h^{-1} [μmol quanta m^{-2} s^{-1}]$^{-1}$ or changing the units of light to Watts from 0.04 to 0.84 mg C [mg Chl *a*]$^{-1}$ h^{-1} [W m^{-2}]$^{-1}$ and P^B_m from 0.73 to 10.50 mg C [mg Chl *a*]$^{-1}$ h^{-1}. α^B and P^B_m were significantly correlated one to another (r_p = 0.73, Fig. 7a). α^B was also significantly correlated with $a^B_{ph}(676)$ ($r_s = 0.49$, Fig. 7b). The photoadaptation parameter, I_k, was significantly correlated to $a^B_{ph}(676)$ ($r_s = -0.41$, Fig. 7c). None of the photosynthetic parameters were correlated to *in situ* SST.

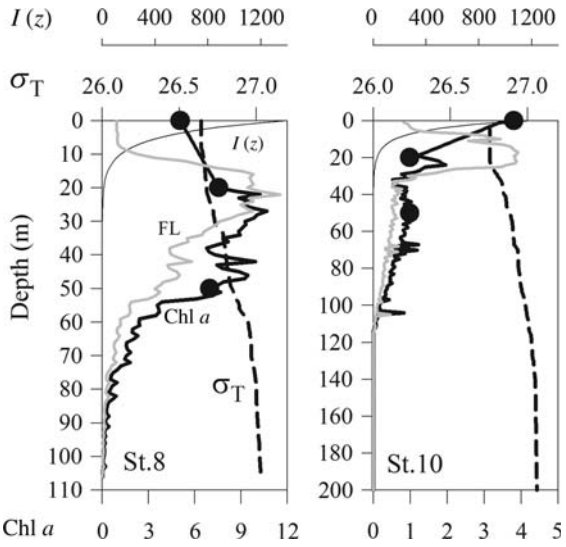

Fig. 6. Vertical profiles of stations 8 and 10 showing evidence of photoinhibition of fluorescence at the surface. The distribution of Chl *a* (mg m^{-3}), *in vivo* fluorescence (relative units), downwelling irradiance ($I(z)$, μmol quanta m^{-2} s^{-1}) and density (σ_T kg m^{-3}) are depicted.

Integrated primary production (field)

Daily water-column integrated primary production, $P_{Z,T}$ showed a wide variation (275–5480 mg C m^{-2} d^{-1}) (Fig. 8a; color image available as Supplementary Data). The highest locations of $P_{Z,T}$ were detected in the north at the shelf-break (up to 5480 mg C m^{-2} d^{-1} at St. 7). High values were also observed in Grande Bay (2899 mg C m^{-2} d^{-1} at St. 71), and at some coastal areas, close to Puerto Deseado and on *Transect V* (up to 2340 mg C m^{-2} d^{-1} at St. 50).

Surface-instantaneous production, $p(0)$, and $P_{Z,T}$ were significantly correlated with surface Chl *a* (Fig. 9a and b). Neither $p(0)$ nor $P_{Z,T}$ were correlated with water-column integrated Chl *a* values. The lack of correlation between the vertical distribution of production and Chl *a* was clearly shown in some profiles (Fig. 10). Integrated $P_{Z,T}$ was significantly correlated with the values of K_d(PAR) at 5 m ($r_s = 0.62$, Fig. 9c). Neither p(0 m) nor $P_{Z,T}$ were correlated to *in situ* SST.

Integrated primary production (satellite)

Maps of satellite modeled daily primary production (Fig. 8b and c; color image available as Supplementary Data) resembled greatly the distribution of satellite-Chl *a* estimations (Fig. 3b and c; color image available as Supplementary Data). Field measurements showed a stronger relationship with daily SeaWiFS-$P_{Z,T}$ modeled

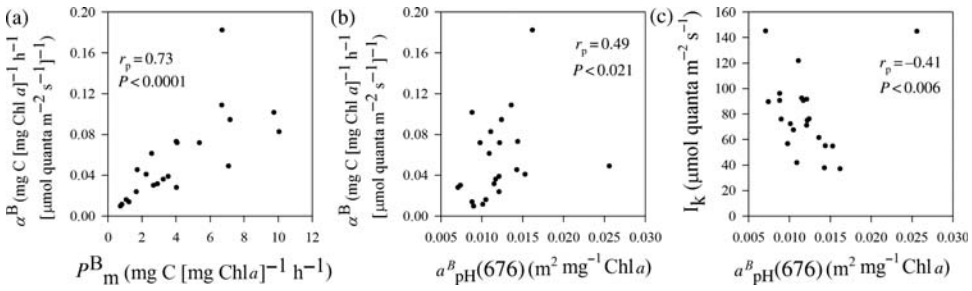

Fig. 7. Correlations between: (**a**) the two photosynthetic parameters [P^B_m vs α^B]; (**b**) the specific absorption coefficient of phytoplankton [$a^B_{ph}(676)$] vs the slope [α^B] and (**c**) the specific absorption coefficient of phytoplankton [$a^B_{ph}(676)$] vs the photoadaptation parameter [I_k]. For all panels $n = 22$.

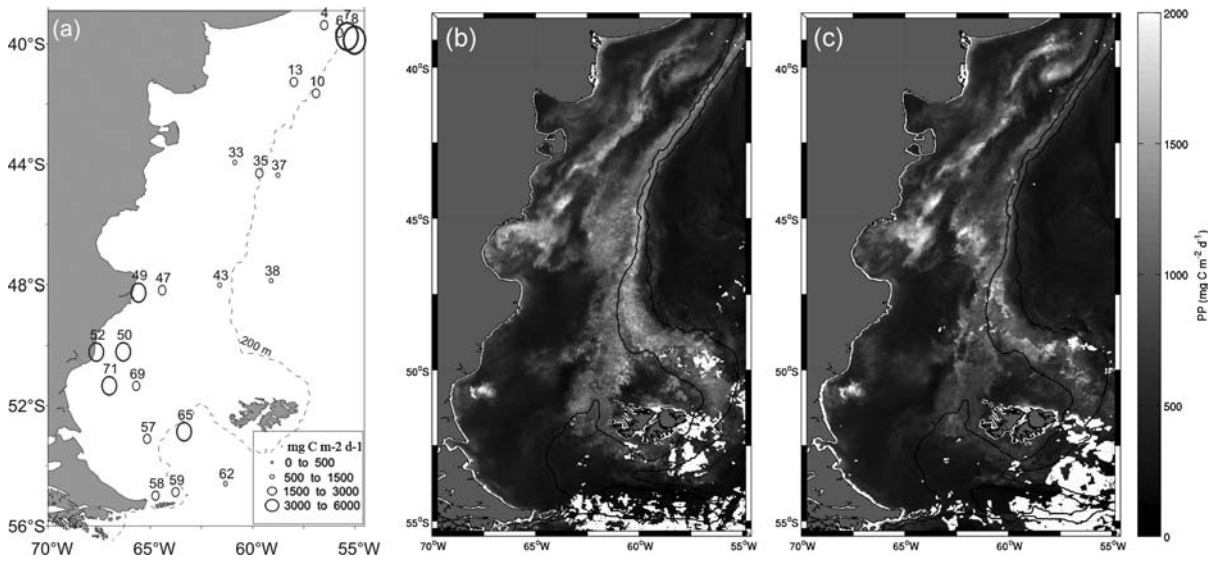

Fig. 8. Distribution of $P_{Z,T}$ (mg C m^{-2} d^{-1}) in the studied area. (**a**) Size-coded circles show the range of values for field estimations at selected stations. Composite satellite estimated $P_{Z,T}$ images for the period of the cruise (8–28 October 2005; see text for details of the models used); (**b**) SeaWiFS; (**c**) MODIS. Dots show the positions of the "match ups" ($N = 4$ for SeaWiFS and $N = 8$ for MODIS).

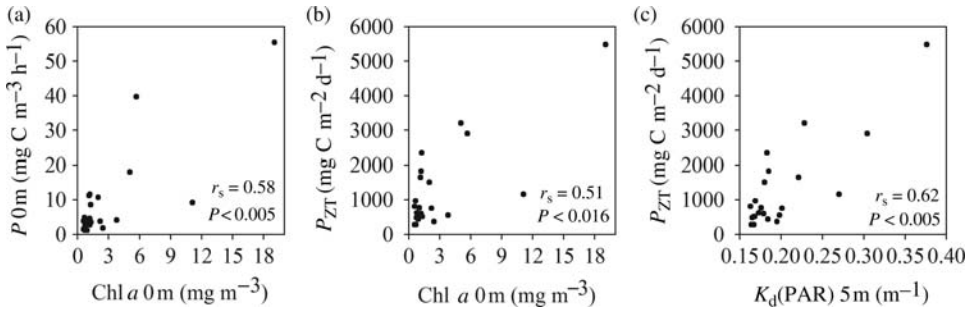

Fig. 9. Correlations between primary production values, Chl *a*, and the attenuation coefficient of light. (**a**) Chl *a* at the surface vs instantaneous production at the surface at noon; (**b**) Chl *a* at the surface vs integrated production [P_{ZT}]; (**c**) K_d(PAR) at 5 m vs integrated production [P_{ZT}]. For all panels $n = 22$.

values than with MODIS-$P_{Z,T}$ values (Table II, Fig. 11a and c). Satellite modeled $P_{Z,T}$ values generally underestimated field ones, especially at high values. The absolute percentage differences (APD) were 50.74% for SeaWiFS and 56.80% for MODIS (Fig. 11, Table II). When the match-up was performed using the composite $P_{Z,T}$ image, satellite values still underestimated field measurements and the uncertainty was approximately 55% (Table II, Fig. 11b and d).

DISCUSSION

Distribution of phytoplankton biomass

The spring blooms developing on the Argentine shelf and shelf-break area during October 2005 confirm the well known richness in phytoplankton biomass of this part of the southwestern Atlantic. The distribution of surface Chl *a* showed high concentrations in several oceanic and coastal frontal systems, as has been already described in previous field (Carreto *et al.*, 2007; Garcia *et al.*, 2008; Reta, in press) and satellite (Rivas *et al.*, 2006; Romero *et al.*, 2006) studies in the region.

Garcia *et al.* (Garcia *et al.*, 2008) proposed that one of the main factors explaining the strong diatom bloom, found in spring 2004 at the Patagonian shelf-break, would be the input of nutrients by upwelling from the Malvinas Current towards the stable shelf waters (Matano and Palma, 2008). However, we found that the bloom at the shelf-break extended in some cases well within the domain of the Malvinas Current; for example at station 8 in transect I [*in situ* temperature (4.362–7.157°C) and salinity values (34.04–34.09)

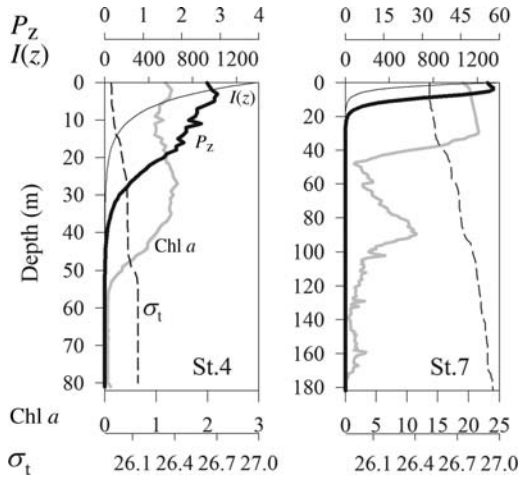

Fig. 10. Vertical profiles of: Chl *a* (mg m^{-3}), primary production at noon [p_Z, mg C m^{-3} h^{-1}], downwelling irradiance at noon [$I(z)$, μmol quanta $m^{-2}s^{-1}$], and density [σ_E kg m^{-3}] for the stations 4 and 7.

Table II: Comparison of field and satellite-modeled P_{ZT} evaluation for SeaWiFS (SW) and MODIS (MD)

Variable	Slope	Intercept	R^2	*N*	RPD	APD
$P_{Z,T}$ (SW)	0.72	0.578	0.97	4	−50.74	50.74
$P_{Z,T}$-composite (SW)	0.77	0.451	0.26	21	−25.09	54.48
$P_{Z,T}$ (MD)*	0.55	1.057	0.34	8	−32.56	56.80
$P_{Z,T}$-composite (MD)	0.63	0.827	0.39	22	−34.79	50.64

Obs: RPD and APD are the mean relative and absolute percentage differences between satellite-derived (X_{sat}) and field (X_{field}) estimates, where X stands for modeled primary production (P_{ZT}) and were calculated as

$$\mathrm{RPD} = \frac{1}{n}\sum_{n=1}^{N}\left(\frac{X_{\mathrm{sat}} - X_{\mathrm{field}}}{X_{\mathrm{field}}}\right) \times 100; \quad \mathrm{APD} = \frac{1}{n}\sum_{n=1}^{N}\frac{|X_{\mathrm{sat}} - X_{\mathrm{field}}|}{X_{\mathrm{field}}} \times 100$$

*All linear correlations were statistically significant ($P < 0.05$), except.

characteristic of Malvinas Current]. The vertical profile of density at this station indicated only a weak stratification, which was due to temperature. Despite the apparent lack of physical stratification the distribution of phytoplankton showed strong vertical variations. The thermal stratification could be caused in part by high solar radiation warming the surface layer (if the rate of vertical mixing was slow enough), but also could be enhanced by phytoplankton itself influencing the heat balance of the ocean (Sathyendranath *et al.*, 1991; Frouin and Iacobellis, 2002).

A conspicuous feature found at station 7 (Fig. 10) was the large biomass of phytoplankton distributed below the euphotic layer (1% $I_o \sim 13$ m). One explanation could be that vertical mixing was strong enough (to bring cells from depth to the lighted layer), but we do not know the rate of physical mixing. On the other hand, the CF ratio showed a clear photoinhibition at the surface; changes in redistribution of energy of this kind are known to occur at short time scales (order ~20 min; Cullen and Lewis, 1988). Hence, a crude estimation would be that physical mixing occurred at a rate that allowed the cells to reside close to the surface for at least 20 min. The effect of vertical mixing on the primary production for different populations of phytoplankton in this region has been reported (Barbieri *et al.*, 2002). This antecedent together with our results, showing signs of vertical acclimation in fluorescence properties, suggests that photosynthetic capacity might have been different with depth as well. The degree of variation in photosynthetic parameters in the water column remains to be studied for this region.

Variations in phytoplankton *in vivo* fluorescence

The efficiency of fluorescence per unit Chl *a* is known to be influenced by the phytoplankton community composition (size and arrangement of the photosynthetic apparatus) and the physiological status of the cells. Kiefer (Kiefer, 1973a) showed that the ratio of *in vivo* to extracted fluorescence varied over one order of magnitude (0.05–0.51) for natural samples; and for the same species (Kiefer, 1973b) according to the nutritional status and time of exposure to different light regimes (e.g. from 0.09 to 0.40). In our study, horizontal variations in CF showed that the efficiency of fluorescence increased at low temperatures (Fig. 5a); although, this relationship was not high showing a large dispersion of points for low values of CF suggesting that other factors contribute to differences in fluorescence efficiency. The relationship with temperature could be partly due to the fact that dissipation of excess energy as heat is expected to diminish at low temperature and hence fluorescence emission increases. Another explanation would be associated with differences in phytoplankton composition in different water masses. The CF ratios were also significantly related to the photosynthetic parameter α^B, indicating that the efficiency of fluorescence per unit Chl *a* would increase as α^B increased; which as discussed in the next section, could be associated with the presence of small size cells.

Another implication of the wide range of CF ratios found is that *in vivo* fluorescence is a poor indication of Chl *a* concentration in this region; and that the use of a single CF factor to convert fluorescence into Chl *a* would have resulted in large errors in Chl *a* (for the

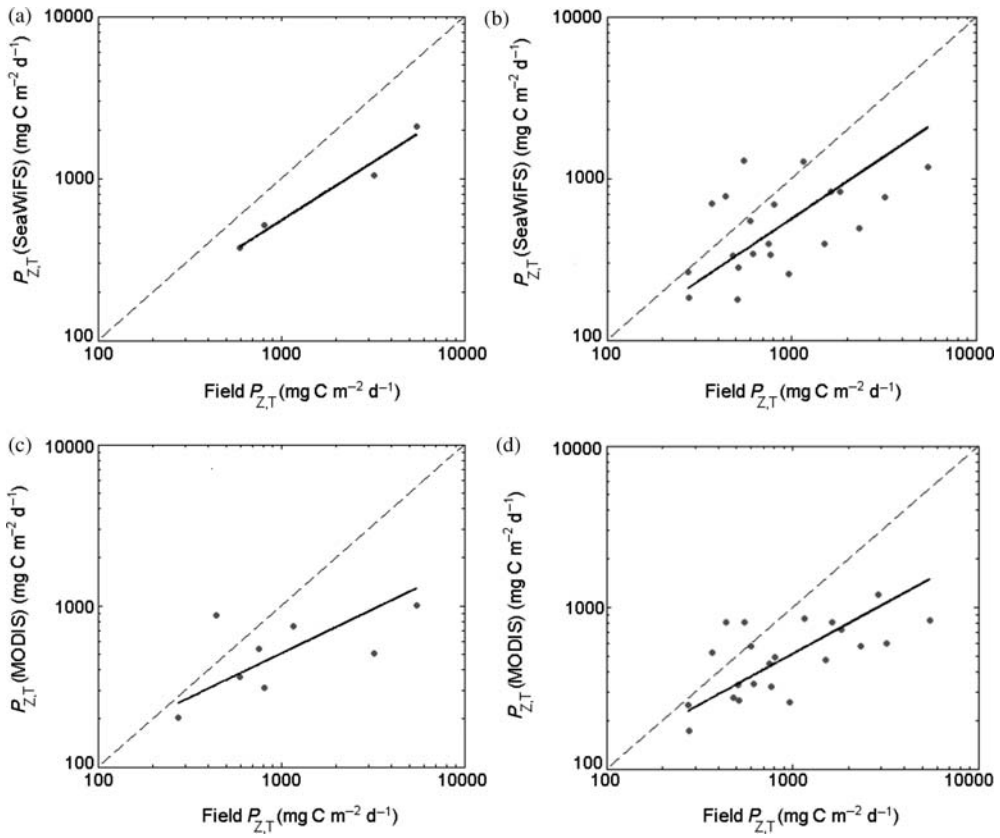

Fig. 11. Relationship between the values of $P_{Z,T}$ (mg C m^{-2} d^{-1}) estimated by field experiments and those estimated by: (**a**) matching SeaWiFS daily $P_{Z,T}$ estimates; (**b**) SeaWiFS composite $P_{Z,T}$ image for the period; (**c**) matching MODIS daily $P_{Z,T}$ estimates; (**d**) MODIS composite $P_{Z,T}$ image for the period. The solid line is the best fit regression line and the dashed line is the 1:1 correlation.

surface APD = 66%, CV = 85%, $n = 132$; for the vertical APD = 70%, CV = 188%, $n = 34$).

The vertical variations in CF showed that the efficiency of fluorescence per unit Chl *a* was higher for high values of the specific absorption coefficient of phytoplankton (Fig. 5c), which could be related to the presence of small cells (Sathyendranath *et al.*, 1999). The photoinhibition of fluorescence at the surface found at some stations indicates, as mentioned previously, that physiological changes occurred at a time scale allowed by the rate of physical mixing. This result also shows the bias produced in some cases by the fluorescence profiles, resulting in a false deep-Chl *a*-maximum (Cullen, 1982).

Variations in the photosynthetic parameters

The values of the photosynthetic parameters estimated in this study (see Results) are close to those reported from a large database of the oceans: α^B from 0.05 to 0.50 mg C [mg Chl *a*]$^{-1}$ h^{-1} [W m^{-2}]$^{-1}$, and for P_m^B from 1.00 to 25.00 mg C [mg Chl *a*]$^{-1}$ h^{-1} (Platt and Sathyendranath, 2009). Benavides (unpublished data) found at stations across the shelf-break (38°–44° S) in spring 1996 values of α^B from 0.06 to 0.50 mg C [mg Chl *a*]$^{-1}$ h^{-1} [W m^{-2}]$^{-1}$, and P_m^B from 0.60 to 27.00 mg C [mg Chl *a*]$^{-1}$ h^{-1}. On the other hand, Villafañe *et al.* (Villafañe *et al.*, 2004) found a narrower range of P_m^B (1.50 and 2.40 mg C [mg Chl *a*]$^{-1}$ h^{-1}) in experiments during late-spring early-summer at the coast (42.7° S). Some differences among these previous and our own results may be due to the different methods used, but part could be due to variations in the phytoplankton communities at the studied locations.

We found a strong correlation between α^B and P_m^B; a common factor intrinsically affecting both parameters would be the species composition of the phytoplankton (Platt *et al.*, 1992). At the same time α^B and I_k were both positively correlated with $a_{ph}^B(676)$, implying that these two photosynthetic parameters increased as cell size decreased. This is because $a_{ph}^B(676)$ indicates variations in the packaging effect; i.e. the efficiency of light absorption in small cells is higher than in larger ones (Duysens, 1956).

These results indicate that in this region the photosynthetic parameters are more influenced by the wide

variations in the composition of the phytoplankton communities (Akselman *et al.*, 2007; Negri and Silva, unpublished results) than by variations in environmental factors. Similar relationships between photosynthetic and bio-optical parameters were found for other regions (Sathyendranath *et al.*, 1999). A more detailed analysis of the relationships between bio-optical and photosynthetic parameters and phytoplankton community composition should be possible in the near future, once taxonomic information from this cruise (studied by local specialists) becomes available. The lack of correlation between photosynthetic parameters and temperature could be due to the complex interaction between phytoplankton types, light regime and nutrient availability in the different water masses (Bouman *et al.*, 2005).

Variations in the field integrated primary production ($P_{Z,T}$)

The range of $P_{Z,T}$ (275–5480 mg C m^{-2} d^{-1}) found was lower than the range of 1900–7800 mg C m^{-2} d^{-1} obtained by Garcia *et al.* (Garcia *et al.*, 2008) also for spring; but they estimated $P_{Z,T}$ only for the shelf-break bloom. On the other hand, our values are higher than those reported by El-Sayed (El-Sayed, 1967) (100–1500 mg C m^{-2} d^{-1}) for the same region and approximately the same season; and by Negri (Negri, 1993) for the April–December period for an area close to the shelf-break at ~39° S of 100–2700 mg C m^{-2} d^{-1}. It should be kept in mind that part of these differences may be due to the different methods used. Regarding differences between the ^{13}C and ^{14}C methods, comparisons carried out in laboratory cultures and natural populations of phytoplankton (Slawyk *et al.*, 1977, 1984) have shown a good agreement between estimates of carbon uptake rates (correlation coefficient 0.91). Other natural causes of variation in production values could be related to interannual changes in the types of phytoplankton present and their physiological state according to availability of nutrients and light.

Variability in surface Chl *a* explained ~50% of the variability for integrated production, and ~60% for surface values (Fig. 9a and b). Therefore, although Chl *a* is a good proxy for phytoplankton biomass (Huot *et al.*, 2007), it offers only a rough indication of primary production in this region. There were no correlations between either integrated or surface values of production and SST. On the other hand, $P_{Z,T}$ was significantly correlated with K_d(PAR) at 5 m (Fig. 9c), which indicates the well-known dependence of production on the light regime.

Satellite modeled production

There are several satellite-based models for estimating primary production (some listed in Behrenfeld and Falkowski, 1997). The standard satellite model used here was chosen given that it follows a similar approach as the model used to estimate field $P_{Z,T}$. However, its estimations showed marked differences from the field ones. Most probably part of it arises from the error in satellite Chl *a* retrieval. A sensitivity analysis of the model inputs showed that chlorophyll concentration is the most significant source of variability in this model estimates of $P_{Z,T}$, thus errors in the satellite-derived Chl *a* product, mainly associated with the presence of waters with different optical characteristics in this region (Moore *et al.*, 2009), will directly influence the modeled $P_{Z,T}$. A comparison between field and satellite derived products for this cruise (not shown here) showed significant correlations between *in situ* and satellite Chl *a* ($r^2 = 0.43$ for SeaWiFS and $r^2 = 0.61$ for MODIS) and that both algorithms underestimated *in situ* data. In particular MODIS OC3M underestimation of *in situ* Chl *a* was higher than SeaWiFS (RPD = −35.4 and −9.16%, respectively). These values of uncertainty are in accordance with those found in previous works in this region (Garcia *et al.*, 2005; Dogliotti *et al.*, 2009), and are close to the minimum expected 35% accuracy for satellite chlorophyll retrieval (Hooker and McClain, 2000).

Other sources of error in satellite $P_{Z,T}$ would be associated with the assumptions of: a uniform biomass distribution with depth, which showed in several stations strong vertical variations; and fixed (temporally and spatially) photosynthetic parameters (Longhurst *et al.*, 1995). Although these parameters fell within the range of those obtained from field estimations, the range was nevertheless wide. Another possible error would be the use of a constant value of K_d(PAR) with depth, estimated from remotely sensed information.

CONCLUDING REMARKS

Surface distribution of *in situ* Chl *a* in the Argentine Sea showed a rich phytoplankton biomass with strong spring blooms. Vertical variations in Chl *a* distribution were notable in several locations, despite the sometimes weak physical stratification.

A large variability was observed in physiological responses of phytoplankton. The Chl *a*/*in vivo* fluorescence ratio showed a wide range. These variations followed a relationship with SST, the type of phytoplankton, its photoacclimation status and photosynthetic

capacity; as indicated by the relationships between CF and $a^B_{ph}(440)$ and α^B. The photosynthetic parameters were far from constant in the region. The relationships found between α^B and P^B_m, as well as between the specific absorption coefficient of phytoplankton with α^B and with I_k, indicate that the distribution of the photosynthetic parameters in this region was influenced by the different types of phytoplankton present.

Field estimations of daily water-column integrated primary production were high and showed a large spatial variability; with the highest values at the north of the shelf-break and Grande Bay. Surface Chl *a* explained only half of this variability. Satellite primary production calculations tend to underestimate these field values (APD > 50%). This was probably due, apart from errors in the satellite Chl *a* retrieval, to the assumptions of the standard model used.

The development of a more suitable satellite model of estimation of primary production for this region should make use of local photosynthetic parameters as well as a parameterization of the vertical distribution of phytoplankton. Better estimates of primary production in this biologically-rich area are required as input for local studies of dynamics of the trophic web (Sabatini *et al.*, 2007), ecosystem based fisheries assessments (Jaureguizar and Milessi, 2008), and CO_2 exchange (Bianchi *et al.*, 2009); as well as for global estimates of carbon budget and climate change research.

SUPPLEMENTARY DATA

Supplementary data can be found online at http://plankt.oxfordjournals.org.

ACKNOWLEDGEMENTS

This work was facilitated by the contribution of many colleagues who provided us instruments, help on board, unpublished data, but mostly useful advices. Among them we wish to thank: R. Akselman, H.R. Benavides, H. Bouman, C. Campagna, M.O. Carignan, J.I. Carreto, Y. Collos, A.D. Cucchi Colleoni, C. Fernandez, R. Frouin, R. Guerrero, G. Harrison, B. Irwin, N. Maggipinto, N.G., Montoya, R.M. Negri, R. Reta, M. Sabatini, R.I. Silva, and O. Ulloa. We are especially indebted to T. Platt and S. Sathyendranath for their advice on primary production modeling. We thank the collaboration of the Captain and crew of the ARA "Puerto Deseado", and the chief scientist A. Piola. The manuscript highly benefited from suggestions by the editors and two anonymous reviewers. We thank NASA and CONAE for satellite data.

FUNDING

This work was financed by INIDEP and grants from: "Fundación Antorchas" (13900-12), PNUDARG02/018 (GEF-B46, -BB12, -BB61), CONICET-PIP-5935, PICT-07-00649; UBA Project X-176; and an IOCCG fellowship to V.S. This is INIDEP contribution # 1568.

REFERENCES

Akselman, R., Ferrario, M. E., Almandoz, G. *et al.* (2007) Distribución y abundancia del microplancton en el talud del Mar Argentino durante la primavera de 2005. *Bol. Soc. Argent. Bot.*, **42**, 183.

Barbieri, E. S., Villafañe, V. E. and Helbling, E. W. (2002) Experimental assessment of UV effects on temperate marine phytoplankton when exposed to variable radiation regimes. *Limnol. Oceanogr.*, **47**, 1648–1655.

Behrenfeld, M. J. and Falkowski, P. G. (1997) A consumer's guide to phytoplankton primary productivity models. *Limnol. Oceanogr.*, **42**, 1479–1491.

Bianchi, A. A., Ruiz Pino, D., Isbert Perlender, H. G. *et al.* (2009) Annual balance and seasonal variability of sea-air CO_2 fluxes in the Patagonian Sea: their relationship with fronts and chlorophyll distribution. *J. Geophys. Res.*, **114**, C03018. doi: 10.1029/2008JC004854.

Bouman, H., Platt, T., Sathyendranath, S. *et al.* (2005) Dependence of light-saturated photosynthesis on temperature and community structure. *Deep-Sea Res.*, **52**, 1284–1299.

Brown, C. W. and Podesta, G. P. (1997) Remote sensing of coccolithophore blooms in the western South Atlantic Ocean. *Remote Sens. Environ.*, **60**, 83–91.

Campagna, C., Quintana, F., Le Boeuf, B. J. *et al.* (1998) Diving behavior and foraging ecology of female southern elephant seals from Patagonia. *Aquat. Mamm.*, **24**, 1–11.

Carreto, J. I., Benavides, H. R., Negri, R. M. *et al.* (1986) Toxic red-tide in the Argentine Sea. Phytoplankton distribution and survival of the toxic dinoflagellate *Gonyaulax excavata* in a frontal area. *J. Plankton Res.*, **8**, 15–28.

Carreto, J. I., Carignan, M. O., Montoya, N. G. *et al.* (2007) Ecología del fitoplancton en los sistemas frontales del Mar Argentino. In Carreto, J. I. and Bremec, C. (eds), *El Mar Argentino y sus recursos pesqueros*. Tomo 5, El ecosistema marino, INIDEP, Mar del Plata, pp. 11–31.

Collos, Y. and Slawyk, G. (1985) On the compatibility of carbon uptake rates calculated from stable and radioactive isotope data: implications for the design of experimental protocols in aquatic primary productivity. *J. Plankton Res.*, **7**, 595–603.

Cousseau, M. B. and Perrota, R. G. (2000) *Peces marinos de Argentina. Biología, distribución y pesca.* INIDEP, Mar del Plata, 167 pp.

Cullen, J. J. (1982) The deep chlorophyll maximum: comparing vertical profiles of chlorophyll-a. *Can. J. Fish. Aquat. Sci.*, **39**, 791–803.

Cullen, J. J. and Lewis, M. R. (1988) The kinetics of algal photoadaptation in the context of vertical mixing. *J. Plankton Res.*, **10**, 1039–1063.

Dogliotti, A. I., Schloss, I. R., Almandoz, G. O. *et al.* (2009) Evaluation of SeaWiFS and MODIS chlorophyll-a products in the Argentinean Patagonian Continental Shelf (38° S–55° S). *Int. J. Remote Sens.*, **30**, 251–273.

Dubinsky, Z., Falkowski, P. G. and Wyman, K. (1986) Light harvesting and utilization by phytoplankton. *Plant Cell Physiol.*, **27**, 1335–1349.

Duysens, L. N. M. (1956) The flattening of the absorption spectrum of suspensions, as compared to that of solutions. *Biochim. Biophys. Acta*, **19**, 1–12.

El-Sayed, S. Z. (1967) On the productivity of the Southwest Atlantic Ocean and the waters west of the Antarctic Peninsula. In Schmitt, W. and Llano, G. A. (eds), *Biology of the Antarctic Seas III. Antarctic Research Series 11*. American Geophysical Society, Washington, pp. 15–47.

Fernandez, C. I., Raimbault, P., Garcia, N. *et al.* (2005) An estimation of annual new production and carbon fluxes in the northeast Atlantic Ocean during 2001. *J. Geophys. Res.*, **110**, C07S13. doi: 10.1029/2004JC002616.

Frouin, R. J. and Iacobellis, S. F. I. (2002) Influence of phytoplankton on the global radiation budget. *J. Geophys. Res.*, **107**, 4377. doi: 10.1029/2001JD000562.

Garcia, C. A. E., Garcia, T. V. M. and McClain, C. (2005) Evaluation of SeaWiFS chlorophyll algorithms in the Southwestern Atlantic and Southern Oceans. *Remote Sens. Environ.*, **95**, 125–137.

Garcia, V. M. T., Garcia, C. A. E., Mata, M. M. *et al.* (2008) Environmental factors controlling the phytoplankton blooms at the Patagonia shelf-break in spring. *Deep-Sea Res.I*, **55**, 1150–1166.

Gonzalez-Silvera, A., Santamaria-del-Angel, E., Garcia, V. M. T. *et al.* (2004) Biogeographical regions of the tropical and subtropical Atlantic Ocean off South America: classification based on pigment (CZCS) and chlorophyll-a (Sea WiFS) variability. *Cont. Shelf Res.*, **24**, 983–1000.

Gregg, W. W., Casey, N. W. and McClain, C. (2005) Recent trends in global ocean chlorophyll. *Geophys. Res. Lett.*, **32**, L03606. doi: 10.129/2004GL021808.

Hama, T., Miyazaki, T., Ogawa, Y. *et al.* (1983) Measurement of Photosynthetic Production of a marine Phytoplankton population Using a Stable 13C Isotope. *Mar. Biol.*, **73**, 31–36.

Hoepffner, N. and Sathyendranath, S. (1992) Bio-optical characteristics of coastal waters: absorption spectra of phytoplankton and pigment distribution in the western North Atlantic. *Limnol. Oceanogr.*, **8**, 1660–1679.

Holm-Hansen, O. and Riemann, B. (1978) Chlorophyll a determination: improvements in methodology. *Oikos*, **30**, 438–447.

Holm-Hansen, O., Lorenzen, C. J., Holmes, R. W. *et al.* (1965) Fluorometric determination of chlorophyll. *J. du Conseil*, **30**, 3–15.

Hooker, S. B. and McClain, C. R. (2000) The calibration and validation of SeaWiFS data. *Prog. Oceanogr.*, **45**, 427–465.

Huot, Y., Babin, M., Bruyant, F. *et al.* (2007) Relationship between photosynthetic parameters and different proxies of phytoplankton biomass in the subtropical ocean. *Biogeosciences*, **4**, 853–868.

Jaureguizar, A. J. and Milessi, A. C. (2008) Assessing the sources of the fishing down marine food web process in the Argentinean-Uruguayan Common Fishing Zone. *Sci. Mar.*, **72**, 25–36.

Jeffrey, S. W. and Humphrey, G. F. (1975) New spectrophotometric equations for determining chlorophylls a, b, c1 and c2 in higher plants, algae and natural phytoplankton. *Biochem. Physiol. Pflanzen*, **167**, 191–194.

Kiefer, D. A. (1973a) Fluorescence properties of natural phytoplankton populations. *Mar. Biol.*, **22**, 263–269.

Kiefer, D. A. (1973b) Chlorophyll *a* fluorescence in marine centric diatoms: responses of chloroplasts to light and nutrient stress. *Mar. Biol.*, **23**, 39–46.

Longhurst, A., Sathyendranath, S., Platt, T. *et al.* (1995) An estimate of global primary production in the ocean from satellite radiometer data. *J. Plankton Res.*, **17**, 1245–1271.

Lutz, V. A., Subramaniam, A., Negri, R. M. *et al.* (2006) Annual variations in bio-optical properties at the 'Estación Permanente de Estudios Ambientales (EPEA)' coastal station, Argentina. *Cont. Shelf Res.*, **26**, 1093–1112.

Lutz, V. A., Barlow, R., Tilstone, G. *et al.* (2007) Report of the In situ component of the 'Plymouth Chlorophyll Meeting and Workshops (Extended Antares Network)'. Sponsored by GOOS, GEO, PML and POGO.18–22 September 2006 .World Wide Web electronic publication. www.antares.ws/publications.

Mandelli, E. F. (1965) Contribución al conocimiento de la producción orgánica primaria en aguas Sub-Antárticas (Océano Atlántico Sud-Occidental). *An. Acad. Bras. Cienc.*, **37**, 399–407.

Matano, R. P. and Palma, E. D. (2008) On the upwelling of downwelling currents. *J. Phys. Oceanogr.*, **38**, 2480–2500. doi: 10.1175/2008JPO3783.

Mitchell, B. G. (1990) *Algorithms for Determining the Absorption Coefficient of Aquatic Particulates Using the Quantitative Filter Technique (QFT)*. SPIE, Ocean Optics X, Orlando, Florida.

Moore, T. S., Campbell, J. W. and Dowell, M. D. (2009) A class-based approach to characterizing and mapping the uncertainty of the MODIS ocean chlorophyll product. *Remote Sens. Environ.*, **113**, 2424–2430.

Morel, A., Huot, Y., Gentili, B. *et al.* (2007) Examining the consistency of products derived from various ocean color sensors in open ocean (Case 1) waters in the perspective of a multi-sensor approach. *Remote Sens. Environ.*, **111**, 69–88.

Negri, R. M. (1993) Fitoplancton y producción primaria en el área de la plataforma bonaerense próxima al talud continental. *INIDEP Inf. Tec.*, **1**, 7.

Negri, R. M., Carreto, J. I., Benavides, H. R. *et al.* (1992) An unusual bloom of *Gyrodinium* cf. *aureolum* in the Argentine sea: community structure and conditioning factors. *J. Plankton Res.*, **14**, 261–269.

Platt, T. and Sathyendranath, S. (1993) Estimators of primary production for interpretation of remotely sensed data on ocean color. *J. Geophys. Res.*, **98**, 14561–14576.

Platt, T. and Sathyendranath, S. (2009) *Light and Marine Primary Production*. Seibutsu Kenkyusha, Tokyo, 174 pp.

Platt, T., Gallegos, C. L. and Harrison, W. G. (1980) Photoinhibition of photosynthesis in natural assemblages of marine phytoplankton. *J. Mar. Res.*, **38**, 687–701.

Platt, T., Sathyendranath, S., Ulloa, O. *et al.* (1992) Nutrient control of phytoplankton photosynthesis in the Western North Atlantic. *Nature*, **356**, 229–231.

Pope, R. M. and Fry, E. S. (1997) Absorption spectrum (380–700 nm) of pure water: II. Integrating cavity measurements. *Appl. Opt.*, **36**, 8710–8723.

Reta, R. (in press) El ecosistema de la plataforma patagónica austral durante el verano (marzo-abril 2000). II. Estimación de la biomasa fitoplanctónica a partir de la distribución de clorofila a. *Rev. Invest. Desarr. Pesq., INIDEP.*

Rivas, A. L., Dogliotti, A. I. and Gagliardini, D. A. (2006) Seasonal variability in satellite-measured surface chlorophyll in the Patagonian shelf. *Cont. Shelf Res.*, **26**, 703–720.

Romero, S. I., Piola, A. R., Charo, M. *et al.* (2006) Chlorophyll-a variability off Patagonia based on SeaWiFS data. *J. Geophys. Res.*, **111**, C0521. doi: 10.1029/2005JC003244.

Sabatini, M., Reta, R. and Matano, R. (2004) Circulation and zooplankton biomass distribution over the southern Patagonian shelf during late summer. *Cont. Shelf Res.*, **24**, 1359–1373.

Sabatini, M., Akselman, R., Reta, R. *et al.* (2007) Estructuración de las comunidades planctónicas e hidrografía en el ecosistema de la Plataforma Patagónica Austral (Argentina). In *XII Congreso Latinoamericano de Ciencias del Mar.* Florianópolis, Brasil. Resúmenes Expandidos. AOCEANO -Associação Brasileira de Oceanografia [CD-ROM].

Sathyendranath, S. and Platt, T. (1988) The spectral irradiance field at the surface and in the interior of the ocean: a model for applications in oceanography and remote sensing. *J. Geophys. Res.*, **93**, 9270–9280.

Sathyendranath, S., Gouveia, A. D., Shetye, S. R. *et al.* (1991) Biological control of surface temperature in the Arabian Sea. *Nature*, **349**, 54–56.

Sathyendranath, S., Stuart, V., Irwin, B. *et al.* (1999) Seasonal variations in bio-optical properties of phytoplankton in the Arabian Sea. *Deep-Sea Res. II*, **46**, 633–653.

Schloss, I. R., Ferreyra, G. A., Ferrario, M. E. *et al.* (2007) Role of phytoplankton communities in the sea-air variation of pCO_2 in the SW Atlantic Ocean. *Mar. Ecol. Prog. Ser*, **332**, 93–106.

Signorini, S. R., Garcia, V. M. T., Piola, A. R. *et al.* (2006) Seasonal and interannual variability of calcite in the vicinity of the Patagonian shelf break (38°S – 52°S). *Geophys. Res. Lett.*, **33**, L16610. doi: 10.1029/2006GL026592.

Slawyk, G., Collos, Y. and Auclair, J. C. (1977) The use of the ^{13}C and ^{15}N isotopes for the simultaneous measurement of carbon and nitrogen turnover rates in marine phytoplankton. *Limnol. Oceanogr.*, **22**, 925–932.

Slawyk, G., Minas, M., Collos, Y. *et al.* (1984) Comparison of radioactive and stable isotope tracer techniques for measuring photosynthesis: ^{13}C and ^{14}C uptake by marine phytoplankton. *J. Plankton Res.*, **6**, 249–257.

Villafañe, V. E., Marcoval, M. A. and Helbling, E. W. (2004) Photosynthesis versus irradiance characteristics in phytoplankton assemblages off Patagonia (Argentina): temporal variability and solar UVR effects. *Mar. Ecol. Prog. Ser.*, **284**, 23–34.

Wright, S. W., Jeffrey, S. W. and Mantoura, R. F. C. (1997) Evaluation of methods and solvents for pigment extraction. In Jeffrey, S. W., Mantoura, R. F. C. and Wright, S. W. (eds), *Phytoplankton Pigments in Oceanography. Monographs on Oceanographic Methodology.* UNESCO, Paris, pp. 261–282.